

129

UNCLASSIFIED

287

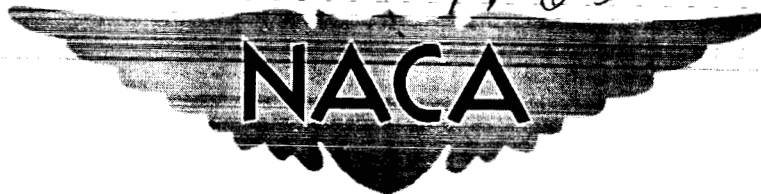
Copy

RM E57C29

NACA RM E57C29

N 63-12908

code 1



# RESEARCH MEMORANDUM

INVESTIGATION OF AN AFTERBURNING RAMJET USING GASEOUS  
HYDROGEN AS FUEL AT MACH NUMBER OF 3.0

By Joseph F. Wasserbauer

Lewis Flight Propulsion Laboratory  
Cleveland, Ohio

## OTS PRICE

XEROX

\$

1.60 ph

MICROFILM

\$

0.80 my

CLASSIFICATION CHANGED  
TO UNCLASSIFIED

AUTHORITY: DECLASSIFICATION  
LETTER DATED JUNE 5, 1962

W.H.L.

CLASSIFIED DOCUMENT - TITLE UNCLASSIFIED

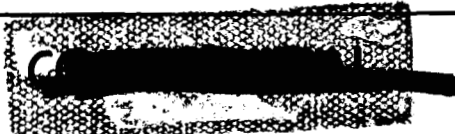
This material contains information affecting the national defense of the United States within the meaning of the espionage laws, Title 18, U.S.C., Secs. 793 and 794, the transmission or revelation of which in any manner to an unauthorized person is prohibited by law.

## NATIONAL ADVISORY COMMITTEE FOR AERONAUTICS

WASHINGTON

June 17, 1957

Reclassified May 29, 1959



U N C L A S S I F I E D

NACA RM E57C29

CONFIDENTIAL

NATIONAL ADVISORY COMMITTEE FOR AERONAUTICS

RESEARCH MEMORANDUM

INVESTIGATION OF AN AFTERBURNING RAMJET USING GASEOUS

HYDROGEN AS FUEL AT MACH NUMBER OF 3.0\*

By Joseph F. Wasserbauer

SUMMARY

An experimental investigation was conducted in the Lewis 10- by 10-foot supersonic wind tunnel on a 16-inch ramjet that was equipped with an afterburner and used gaseous hydrogen for both the primary and afterburner fuels. The primary nozzle had a contraction ratio of 0.6 while the exit nozzle had a contraction ratio of 0.9. Data were obtained at a free-stream Mach number of 3.0 and zero angle of attack.

The results of this investigation illustrate that at a constant diffuser-exit Mach number afterburner operation produces more than twice the thrust available without afterburning. An over-all combustion efficiency of 77 percent with a specific fuel consumption of 0.98 and a specific impulse of 3680, based on net internal thrust, was obtained with afterburning.

INTRODUCTION

Successful afterburning in a 16-inch ramjet with large thrust increases without the necessity of exit nozzle-throat area variation was reported in reference 1. However, the combustion efficiency was rather low. Propylene oxide was used as both the primary and afterburner fuels in the tests of reference 1, and it was concluded that in order to make the ramjet afterburner practical, fuels having greater reaction rates and burning with higher efficiencies are necessary. Recent work with hydrogen (refs. 2 and 3) indicates that this fuel might provide the answer to a practical afterburning ramjet.

An investigation was therefore undertaken to evaluate the performance of a hydrogen-fuel ramjet equipped with an afterburner. The investigation was conducted in the Lewis 10- by 10-foot supersonic wind tunnel at a free-stream Mach number of 3.0 and zero angle of attack.

---

\*Title, Unclassified.

CONFIDENTIAL

The engine was a 16-inch-diameter ramjet previously used in the study of hydrogen as a primary burner fuel (ref. 3). The results obtained are presented and discussed herein.

## SYMBOLS

- $A_{\max}$  maximum frontal area of model (16-in. diam.)
- $C_{F_n}$  net-internal-thrust coefficient (based on max. model area),  
 $F_n/q_0 A_{\max}$
- $F_n$  net internal thrust (exit momentum - free-stream momentum)
- $f/a$  fuel-air ratio
- $l$  length of diverging section of primary nozzle
- $M$  Mach number
- $P$  total pressure
- $p$  static pressure
- $q_0$  free-stream dynamic pressure
- $sfc$  specific fuel consumption based on net internal jet thrust,  $w_f/F_n$
- $x$  static tube location on diverging section of primary nozzle
- $x/l$  ratio of static-pressure tube location to over-all length of diverging section of primary nozzle
- $w_f$  fuel flow, lb/hr
- $\eta_B$  combustion efficiency,  $\frac{\text{Final enthalpy} - \text{Initial enthalpy}}{\text{Available heating value}}$

## Subscripts:

- $p$  primary
- $s$  secondary
- $0$  free-stream conditions
- $2$  airflow measuring station (model station, 65 in.)
- $3$  diffuser-exit station (model station, 108.125 in.)

U N C L A S S I F I E D

### APPARATUS AND PROCEDURE

A schematic diagram of the 16-inch-diameter ramjet engine equipped with the afterburner used in this investigation is shown in figure 1. Also illustrated is a cross section of the ramjet showing the primary nozzle and afterburner fuel injectors. The tests were conducted in the Lewis 10- by 10-foot supersonic wind tunnel at a free-stream Mach number of 3.0 and zero angle of attack at a simulated pressure altitude of 71,000 feet. The tunnel total temperature was  $664 \pm 8^\circ \text{R}$ .

The supersonic inlet, subsonic diffuser, and primary injector are the same as those of reference 3. The afterburner injectors, which had an airfoil cross section, were located 0.50 inch downstream of the converging-diverging primary nozzle. Eight injectors of two different lengths were placed  $45^\circ$  apart. For some of the tests the large injectors were removed. The primary nozzle had a contraction ratio of 0.6 while the afterburner-exit nozzle had a contraction ratio of 0.9. The primary nozzle was sharp-edged at the throat section with a  $15^\circ$  divergent angle. The length of the primary combustor was 26.75 inches measured from the point of fuel injection to the beginning of the converging section of the primary nozzle. The length of the afterburner was 25.75 inches measured from the end of the diverging section of the primary nozzle to the beginning of the exit nozzle. Neither length was varied during the operation. A spark plug was not needed for ignition in the afterburner since the source of ignition of the afterburner fuel was the hot gas from the primary combustor.

Fuel for the primary burner was ducted through the centerbody, and, for convenience in fabrication, fuel for the afterburner was introduced through a system of pipes located outside the model (fig. 1). A photograph of the ramjet afterburner and fuel system is shown in figure 2. The hydrogen fuel was stored as a gas in cylinder tanks at a pressure of 2400 pounds per square inch gage. Fuel was taken directly from the storage cylinders through a pressure-reducing valve, two metering orifices (for afterburner and primary fuel flows), and a throttling valve to the engine.

Mass flow entering the inlet was calculated in the same manner as reported in reference 3. Diffuser static and total pressures were measured at the pressure survey rake station indicated on figure 1. Exit total pressure was measured with a water-cooled tail rake located immediately after the exhaust nozzle. Net internal thrust (exit momentum minus free-stream momentum) was then calculated from the exit total pressure. The exit total temperature was also calculated from the measured exit total pressure and continuity relation. Combustion efficiency  $\eta_B$  was calculated from the enthalpy rise of the gas through the primary-combustor and afterburner sections divided by the available heat content of the fuel.

In the method used for calculating  $\eta_B$ , no account was made of changes in gas properties accompanying combustion efficiencies less than 100 percent. A check using a more refined procedure indicates that burner efficiencies would appear somewhat lower than those presented. For example, at a recorded burner efficiency of 74 percent, calculation by the refined method would reduce the apparent efficiency to 70.5 percent. This apparent error in  $\eta_B$  would increase in proportion to the decrease in calculated  $\eta_B$  below 100 percent. However, compensating errors due to thermal expansion of the nozzle-discharge area and to heat losses through the engine shell were not included in the analysis. Hence, the combustion efficiencies presented are believed more representative than those that would be obtained from the refined analysis.

A static-pressure survey of the gas flowing into the afterburner was made on the diverging side of the primary nozzle just after the primary throat as shown in figure 1.

During afterburner operation the inlet was maintained at the same operating point by sensing the normal shock by means of a backward-facing total-pressure probe located 6.5 inches downstream of the cowl lip. The shock position was regulated by varying the primary-burner fuel flow as afterburner fuel flow was varied.

## RESULTS AND DISCUSSION

The diffuser performance of the 16-inch ramjet engine equipped with an afterburner is the same as that reported in reference 3. The inlet operating point ( $M_3 = 0.185$ ;  $P_2/P_0 \approx 0.50$ ) was held slightly supercritical for convenience in avoiding buzz.

In reference 1 afterburner operation was accomplished by keeping the diffuser conditions constant. However, in order to keep a constant diffuser operating condition during the present test, the primary-combustor fuel flow had to be varied because the primary nozzle appeared to be unchoked. Since the presence of the afterburner fuel injectors might account for this, tests were made with the four large injectors removed. Data showing the resulting wall static pressures measured in the divergent part of the nozzle are presented in figure 3. For the no-burning case (fig. 3(a)), it appears that the primary nozzle is choked with the flow probably separated. A rise in static pressure, which was reduced by removal of the large injectors, occurred near the end of the diverging section. With the primary burner in operation (fig. 3(b)), removal of the large afterburner injectors appears to have a marked effect in reducing the wall static pressure. During afterburner operation (fig. 3(c)), the primary nozzle is unchoked at the high afterburner fuel-air ratios and probably at the low fuel-air ratios. Again, the removal of the large

injectors reduced the wall static pressure at both the high and low fuel-air ratios. The wall static pressures were constant along the length for the high and low afterburner fuel-air ratios with the large injectors removed. A possible explanation of this might be propagation and burning of the afterburner fuel forward into the separated region of the nozzle.

In reference 1 the diffuser-exit Mach number was slightly reduced as the afterburner fuel flow was increased, probably because of the method of afterburner fuel injection. In this investigation the effect was more pronounced even though fuel was not injected ahead of the primary nozzle. The primary fuel flow was decreased in order to keep the diffuser operating condition constant while increasing afterburner fuel flow. Large increases in net internal thrust were obtained with afterburner operation.

The net-internal-thrust coefficient with and without ramjet afterburning is shown in figure 4. For primary-burner operation only, the data were obtained with the afterburner configuration cut off at the primary nozzle throat in order to measure the total pressure at this point. Operation with only the primary burner and nozzle gave a net-internal-thrust coefficient of nearly 0.6 at the diffuser-exit Mach number used for operation of the afterburner.

For afterburner operation the net-internal-thrust coefficient increased from 0.6 to 1.285. This is more than twice the thrust available with only the primary burner in operation. Even greater increases in thrust can be realized with the employment of larger exit nozzles.

Variations of fuel-air ratio, combustion efficiency, and specific fuel consumption with the net-internal-thrust coefficient for these data are shown in figure 5. Without afterburner operation the peak thrust coefficient of 0.6 reached corresponds to a combustion efficiency of 83 percent and a specific fuel consumption of 0.84 (based on net internal thrust).

During afterburner operation, a peak combustion efficiency of 77 percent was achieved with an increase in thrust coefficient of 83 percent at this point in afterburner operation. The corresponding specific fuel consumption was 0.98. Further increases in heat addition (increasing fuel-air ratio) resulted in a thrust increase of more than twice that obtained without afterburning but at reduced combustion efficiency and higher specific fuel consumption. The drop in burning efficiency at the higher thrust levels can be largely attributed to the reduced temperatures at the primary nozzle necessary to keep the inlet at the desired operating point.

It is of interest to compare the specific impulse (based on net internal thrust) of a booster rocket to that of the ramjet afterburner. For the ramjet afterburner a maximum specific impulse of 3680 was obtained as compared with a representative value of about 300 for a booster rocket.

Although the mode of operation was not as described in reference 1 because of unchoking of the primary nozzle, it was demonstrated that the ramjet afterburner can efficiently provide large thrust increases. If a way could be found to avoid this unchoking, higher over-all combustion efficiencies could be attained at maximum thrust, and the problem of scheduling primary fuel-air ratio with thrust level could be eliminated.

### SUMMARY OF RESULTS

The following results were obtained during an investigation in the Lewis 10- by 10-foot supersonic wind tunnel at a Mach number of 3.0 of ramjet afterburning with gaseous hydrogen as fuel.

1. At a constant diffuser-exit Mach number afterburner operation produced more than twice the thrust available as compared to operation without afterburning.
2. Over-all combustion efficiencies as high as 77 percent were obtained with afterburning.
3. With afterburning a specific fuel consumption of 0.98 and a specific impulse of 3680, based on net internal thrust, were obtained.

Lewis Flight Propulsion Laboratory  
National Advisory Committee for Aeronautics  
Cleveland, Ohio, April 1, 1957

### REFERENCES

1. Perchonok, Eugene, and Wilcox, Fred A.: Investigation of Ram-Jet Afterburning as a Means of Varying Effective Exhaust Nozzle Area. NACA RM E52H27, 1952.
2. Silverstein, Abe, and Hall, Eldon W.: Liquid Hydrogen as a Jet Fuel for High-Altitude Aircraft. NACA RM E55C28a, 1955.
3. Wasserbauer, Joseph, F. and Wilcox, Fred A.: Combustor Performance of a 16-Inch Ram Jet Using Gaseous Hydrogen as Fuel at Mach Number 3.0. NACA RM E56K28a, 1957.

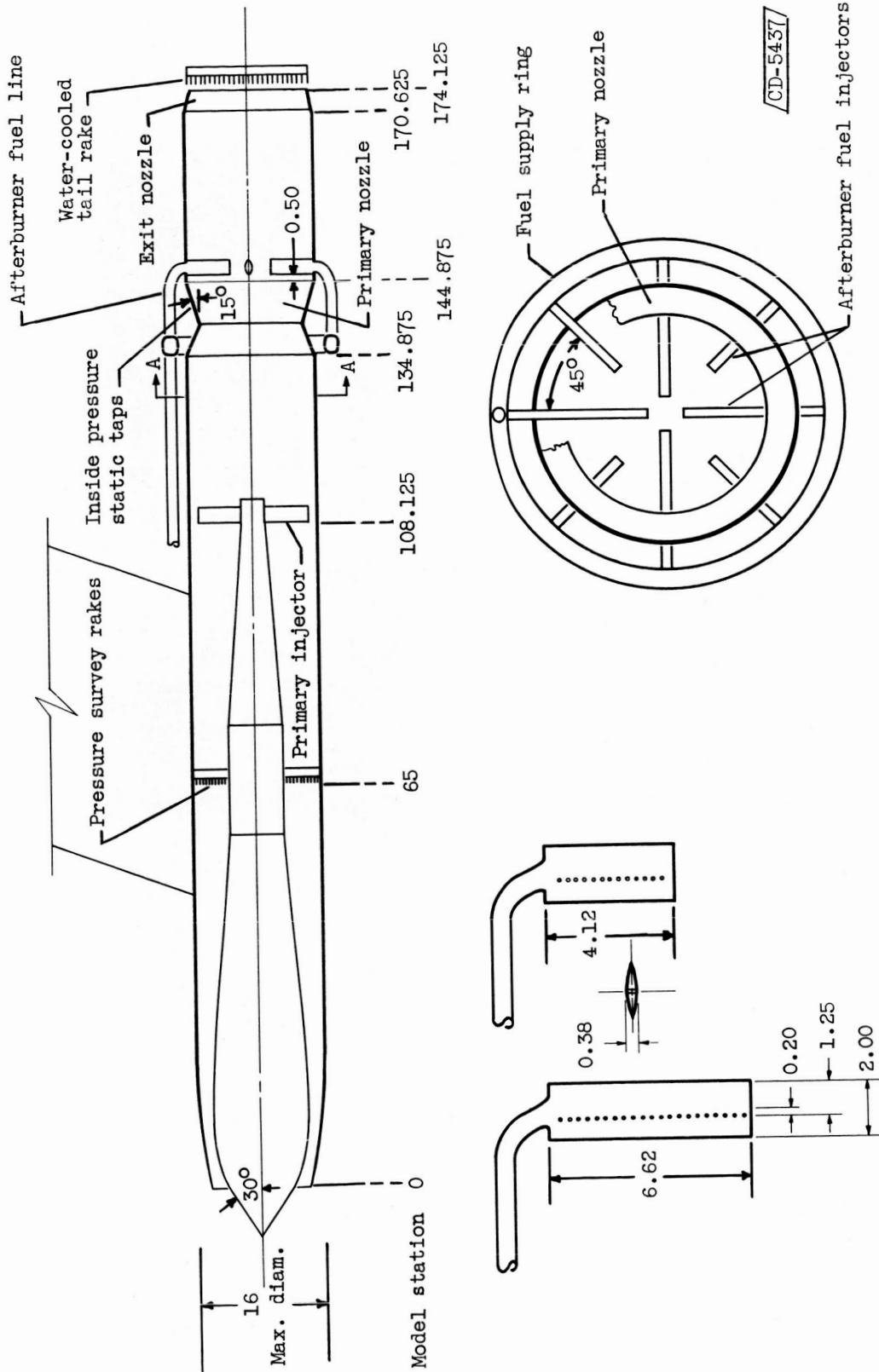


Figure 1. - Model of 16-inch ramjet afterburner and details. (All dimensions in inches except where noted.)





Figure 2. - Afterburner and afterburner fuel system.

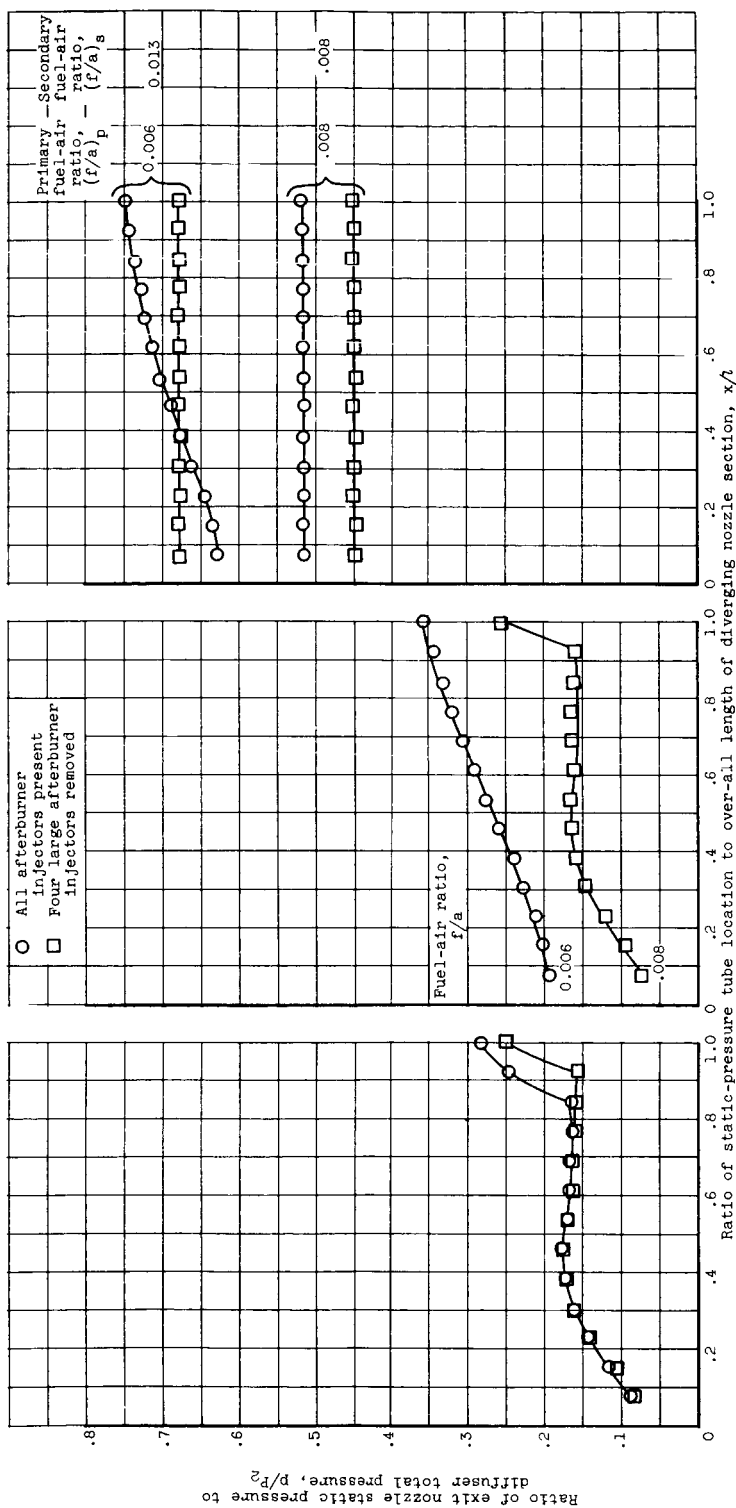


Figure 3. - Static-pressure variation along diverging section of primary nozzle for different test conditions.  
(a) No burning.  
(b) Primary burner in operation only.  
(c) Afterburner operation.

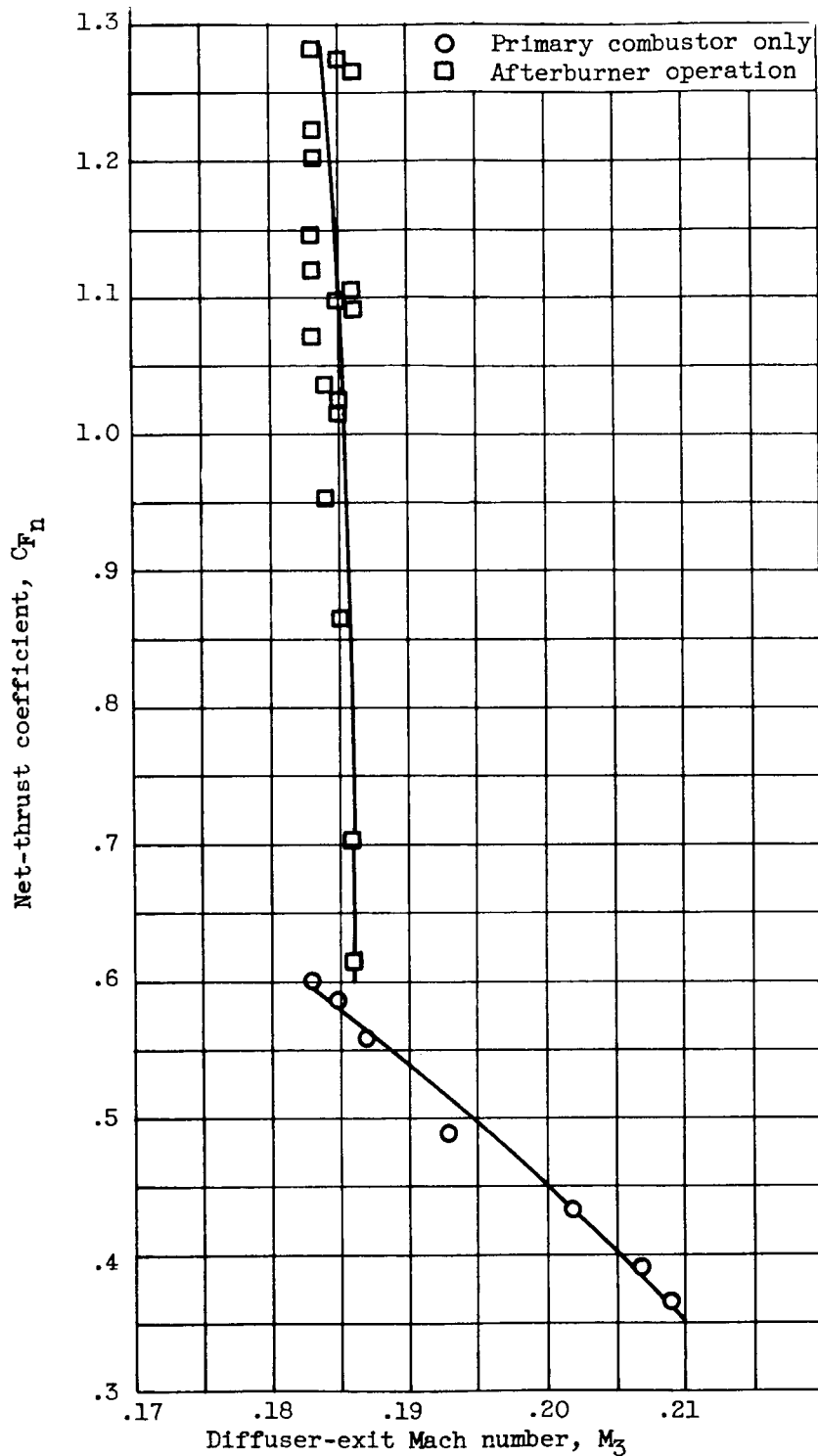


Figure 4. - Variation of net-thrust coefficient with and without afterburning. All afterburner fuel injectors present.

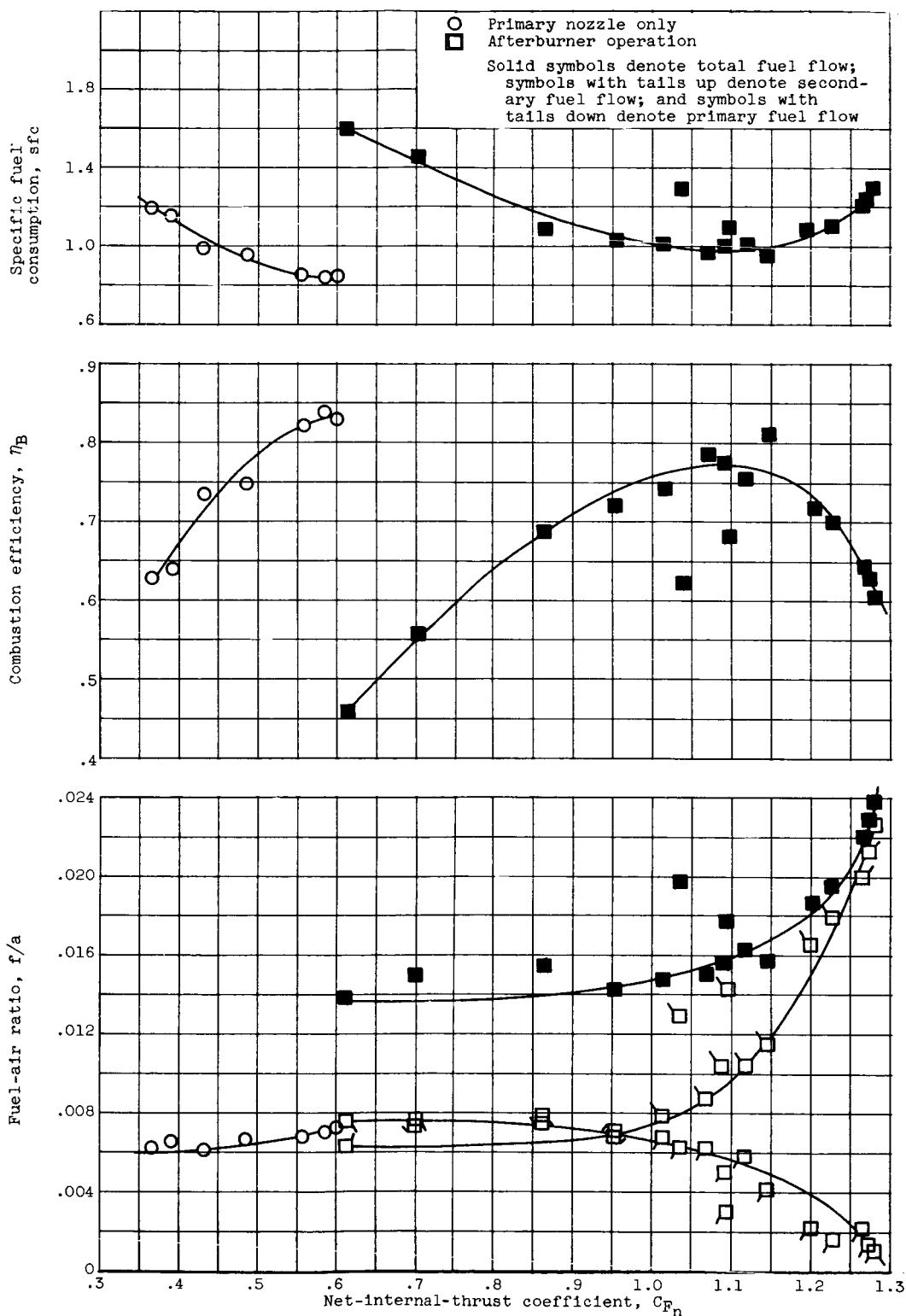


Figure 5. - Variation of net-internal-thrust coefficient with fuel-air ratio, combustion efficiency, and specific fuel consumption. All afterburner injectors present.